Magazine of Civil Engineering. 2020. 98(6). Article No. 9802

Magazine of Civil Engineering

ISSN 2712–8172

journal homepage: http://engstroy.spbstu.ru/

DOI: 10.18720/MCE.98.2

Mechanical-thermal characteristics of foamed ultra-lightweight composites

T.-P. Huynh*[a], *N.-T. Ho*[b], *P.-T. Bui*[c,d], *N.-D. Do*[e], *T.-C. Nguyen*[f]**

[a] *Can Tho University, Can Tho City, Viet Nam*

[b] *VSB Technical University of Ostrava, Ostrava, Czech Republic*

[c] *Ho Chi Minh City University of Technology, Ho Chi Minh City, Viet Nam*

[d] *Viet Nam National University Ho Chi Minh City, Ho Chi Minh City, Viet Nam*

[e] *National Taiwan University of Science and Technology, Taipei City, Taiwan*

[f] *Le Quy Don Technical University, Ha Noi City, Viet Nam*

** E-mail: htphuoc@ctu.edu.vn*

Keywords: composite, cement, fly ash, compressive strength, thermal behavior, microstructure

Abstract. Turning waste into construction materials recently gets much attention from the researchers in the world due to the advantages of not only the eco-friendly environment but also the positive enhancement of material characteristics. Thus, this study investigates the feasibility of the use of a ternary mixture consisting of cement, ground granulated blast-furnace slag (GGBFS), and fly ash (FA) for producing foamed ultra-lightweight composites (FULC) with the designed dry density of approximately 700 kg/m^3. The FULC specimens were prepared with various FA/GGBFS ratios (16/24, 20/20, and 24/16) and foaming agent/water ratios (1/60, 1/80, 1/100, and 1/120). The constant water-to-binder ratio of 0.2, cement content of 40 % by mass, and superplasticizer dosage of 0.2 % by mass were applied for all FULC mixtures. Properties of the FULC specimens were evaluated through laboratory tests of compressive strength, dry density, thermal conductivity, water absorption, and thermal behavior following the relevant ASTM standards. Additionally, both the microstructure observation and cost analysis of all FULC mixtures was performed. Test results show that reducing GGBFS content resulted in a reduction in the compressive strength, dry density, thermal conductivity, and cost of the FULC. A similar trend could be observed when reducing the concentration of foam in the FULC mixtures. As the results, the 28-day compressive strength, dry density, thermal conductivity, water absorption, and cost of the FULC were in the ranges of 4.41–5.33 MPa, 716–729 kg/m^3, 0.163–0.182 W/mK, 41.5–48.5 %, and 15.3–20.9 USD/m^3, respectively. Furthermore, the FULC exhibited excellent performance under fire conditions as the maximum temperature at the internal surface of the FULC and the normal brick walls were 122 °C and 318 °C after 120 minutes of firing, respectively. Consequently, both GGBFS and FA had enormous potential for the production of FULC.

1. Introduction

Vietnam is facing the demand for housing because of the increase in population density, while the land for construction is limited. That is the reason for the existence of high-rise buildings or skyscrapers, which solves the issues involving human shelter as well as land use. On account of these problems, the solutions are pointed to resolve the situation that buildings have to face up to the heavy-weight and such things as comfort. Foam concrete (FC) is invented to serve sustainable development and respond the human life, and FULC is one of the possible products involving to FC. FC is known as durable, lightweight construction materials, which provide the construction industry lots of advantages by decreasing cost, insulation capacity, and fire resistance of structures [1].

On the other hand, the cost of materials is crucial concerned having a significant effect on the construction; it occupies nearly 60 % of the total cost of building construction [2]. The using of FC can

Huynh, T.-P., Ho, N.-T., Bui, P.-T., Do, N.-D., Nguyen, T.-C. Mechanical-thermal characteristics of foamed ultra-lightweight composites. Magazine of Civil Engineering. 2020. 98(6). Article No. 9802. DOI: 10.18720/MCE.98.2

replace a brick wall to lighten the weight of the building and to cheapen the foundation cost. The smooth surface of foam concrete reduced the cost for plastering as well as construction price. Moreover, the lowering of the air-conditioning cost is in parallel with the reduction of heat flow [3]. Containing an amount of pore (having a total volume of at least 20 %) and having a lot of artificial air-void trapped inside its specimens by using a suitable foaming agent are the excellent characteristics of FULC [4, 5]. The use of FULC provides impressive performance to the building, for the structure of FULC create insulations from heat and act as sound-proof [1]. It is well-known as perfect, an insulating material that is going to hit wide distribution in construction.

Nowadays, scientists have been investigating the enhancement of FULC properties to find out and maximize the application. That FULC productions have been using day by day, the scientific research on FULC will continue to exploit its characteristics to improve construction development. There are ranges of scientific journals that investigate the production of FULC, to mention that FC has advantages of thermal insulation properties, fire-resistant, and durability [6−8]. The idea of increasing the level of thermal protection and improving the humidity regime using a wall made of lightweight materials has been well-applied by Russian researchers [9, 10]. Thus, FULC is invented to serve sustainable development and respond the human life. Having said that FULC is a potential material that can multiply research to discover the leading topic. In spite of the application are widening, the production of FULC gradually become tougher, which is due to the scarcity of input material such as cement. The issues related to cement production are becoming seriously because of environmental problems. Currently, the world's annual demand uses more than 4 billion tons of cement [11], not mentioned it exhaust approximately (5 % CO_2) [12] to the environment. Coupled with the growth of the industry, the ongoing conduct of research topics on using industrial waste to minimize a substantial environmental agent and maximize the production of construction material has been continuing. These studies on FC by using industrial waste that can be mentioned such as the addition of ultrafine GGBFS provided an increase in the compressive strength of FC when using GGBFS as partial cement replacement [13] or the substitution of sand by FA in FC mixes lower foam volume because of FA fineness [14].

This investigation focuses on the combination of blended binders, including FA, GGBFS, and ordinary Portland cement (OPC) to manufacture and aim to assess the characteristics of FULC. The topic thereby contributes to the science of FULC in particular and concrete in general.

2. Materials and Methods

2.1. Materials

Type-I OPC conforming to ASTM C150, GGBFS conforming to ASTM C989, and FA conforming to ASTM C618 were used as the binder materials in this study. Specific gravities and chemical compositions of cement, GGBFS, and FA are listed in Table 1.

As can be seen, cement and GGBFS comprised CaO and SiO_2 majorly, whereas high content of SiO_2 and Al_2O_3 was found in FA. Fig. 1 shows the particle size distribution of GGBFS and FA. Fig. 2 shows the morphology of raw materials consisting of GGBFS and FA by using scanning electron microscopic (SEM). It can be seen that GGBFS had irregular shapes, while FA contained a lot of spherical particles with different sizes.

Table 1. Specific gravity and chemical compositions of raw materials.

Properties		Cement	GGBFS	FA
Specific gravity		3.15	2.92	2.26
Chemical composition (wt.%)	SiO_2	20.0	35.6	55.3
	Al_2O_3	4.2	11.3	22.7
	Fe_2O_3	3.1	0.5	5.9
	CaO	62.4	41.0	5.7
	MgO	4.2	6.5	1.6
	K_2O	0.4	0.6	1.5
	Na_2O	0.3	0.3	3.8
	L.O.I*	1.75	4.71	2.74

*L.O.I – loss on ignition

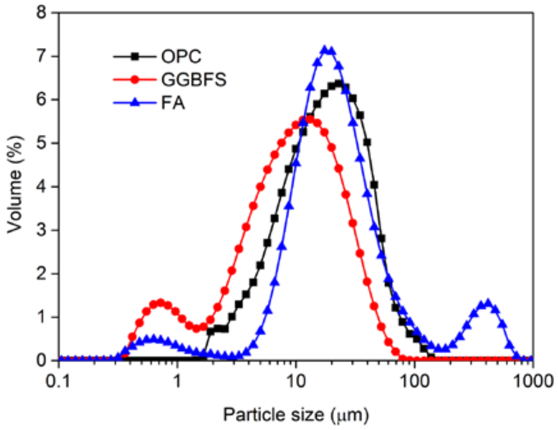

Figure 1. Particle size distribution of raw materials.

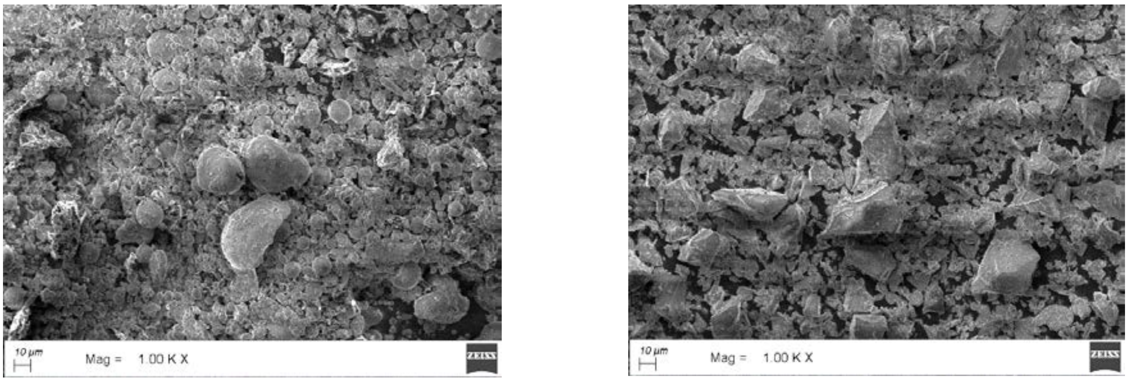

(a) FA **(b) GGBFS**

Figure 2. SEM images of raw materials.

The mineralogical compositions of GGBFS and FA were determined by using X-ray diffraction (XRD), as shown in Fig. 3. The non-crystalize phase existed in the GGBFS structure without any peak whereas the high intensity of quartz was found in FA, which is considered as crystalize phase.

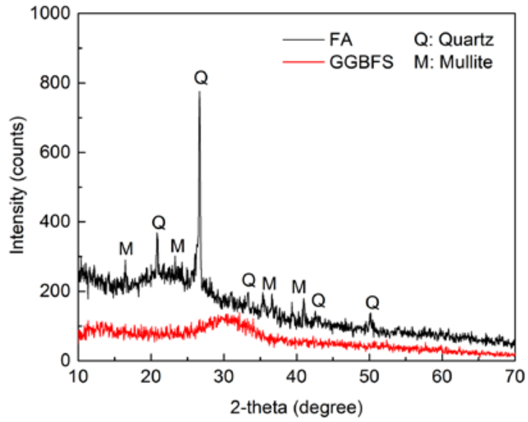

Figure 3. XRD patterns of raw materials.

In this study, the pale brown liquid EABASSOC foaming agent with a specific gravity of 1.02 and pH (in solution) of 6.7 and type-G superplasticizer (SP) sourced from China with a specific gravity of 1.34 were used for the preparation of FULC samples.

2.2. Mixture proportions

Six mixture proportions are prepared in this study, as shown in Table 2. Constant percentages of foam, water, and SP contents were 5, 16, and 0.2 % by mass of FULC, respectively. The content of 40 % cement by weight of FULC was kept constant to assess the influence of FA and GGBFS on properties of FULC. The proportions of FA and GGBFS were in the range of 16–24 % by mass of FULC. It was reported that the foaming agent/water (F/W) ratio affects the formation of the void and porosity of FULC. Therefore, the F/W ratios of 1/60, 1/80, 1/100, and 1/120 were prepared to evaluate the effects of the F/W on the characteristics of FULC.

Table 2. Mixture proportions of FULC.

Materials	% by mass					
	M1	M2	M3	M4	M5	M6
Cement	40	40	40	40	40	40
FA	16	20	24	20	20	20
GGBFS	24	20	16	20	20	20
Foam	5	5	5	5	5	5
Mixing water	16	16	16	16	16	16
SP	0.2	0.2	0.2	0.2	0.2	0.2
F/W*	1/80	1/80	1/80	1/60	1/100	1/120

*F/W − foaming agent-to-water ratio

2.3. Mixing procedure and specimen preparation

All of the materials were kept in anti-moisture bags to prevent the moisture before mixing. The foam was initially generated from different F/W ratios (as shown in Table 2) using a foam generator. After making the foam, the mixing procedures can be started as follows: Firstly, cement, FA, and GGBFS were dry mixed uniformly in a laboratory mixer for 1 min. Mixing water with SP was then gradually added to the dry mixture and allowed to mix for 2 min to obtain a uniform fresh mixture. Finally, the foam was added to the fresh mixture and mixed for another 2 min to get a homogenous fresh paste.

After mixing, the fresh pastes were cast in 50-mm-per-side cube-shaped molds, as seen in Fig. 4. The surfaces of the specimens were then sealed with plastic films to avoid water loss. All specimens were de-molded for 24 h after casting and cured in water until the designated test ages. The finished products were put in laboratory conditions and remolded after 24 h. Right that, all FULC specimens were cured at room condition until the day of testing.

Figure 4. FULC specimens.

2.4. Test methods

Compressive strength of FULC specimens was tested at the ages of 3, 7, 14, and 28 days according to ASTM C109, which can be considered as the modified standard for testing compressive strength of the prepared 50×50×50 mm FULC specimens.

After the compression test, the small pieces obtained from the broken FULC specimens were used for analyzing their microstructure by scanning electron microscopy (SEM). The experiment was performed following the guidelines of Hwang and Huynh [15]. In addition, density, water absorption, and voids of specimens were measured per ASTM C642. The thermal conductivity (TC) was recorded using a portable device model ISOMET 2014 as described by Hwang and Tran [16] to measure the correlation between density and porosity as well as the voids inside FULC.

It is noted that three specimens of each FULC mixture were subjected to each test, and the average value of the three specimens was reported.

2.5. The temperature distribution in the wall by a finite element model

Heat transfer through walls is the energy transmission process that involves objects having different temperatures. The heat transfer typically goes following three different patterns, including heat conduction, heat convection, and thermal radiation. Therefore, modeling of heat transfer must consider the whole solid bodies of a wall, as well as the convection and radiation between the substantial mass of the wall and the external heating sources [17].

Basic equations of heat transfer as described in equation (1) [18, 19]:

$$\lambda \nabla^2 T = \rho c \frac{\partial T}{\partial t}, \tag{1}$$

where: λ is the thermal conductivity, W/(m.K); c is the specific heat, J/(kg.K); ρ is the density, kg/m^3; $\nabla^2 T$ = *div(grad T)* is the Laplace temperature operator.

A variety of boundary conditions, including temperature conditions, heat flow conditions, convection boundary conditions, radiation boundary conditions is often solved in heat transfer analysis. In this study, temperature conditions and convection boundary conditions were used as boundary conditions to solve the problem of heat transfer and equation (2) can be described as follows [20]:

$$q_c = h\left(T_c - T\right), \tag{2}$$

where: $T_c = T_c(t)$ is the temperature of the convective medium, °C; $T = T(t)$ is the temperature of the solid surface, °C; h is the convection coefficient, W/(m^2.K).

The wall of size 3.3×1.1×0.1 m was modeled in ANSYS APDL software. The specific heat, thermal conductivity, and density of brick walls were given as a function of temperature in the range $20 \le T \le 1200$ °C. For simplicity in computational analysis, according to studies [21–23], this simulation assumes the average value of specific heat, thermal conductivity, and density, as given in Table 3. The temperature profile of the wall was plotted by exposing the wall to the standard fire curve ISO 834, as shown in Fig. 5.

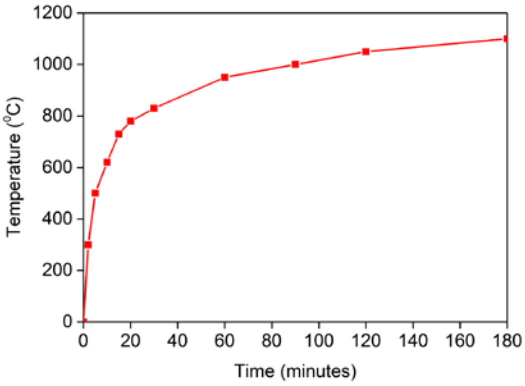

Figure 5. Temperatures versus time curves of standard fire curve ISO 834.

Table 3. Material properties.

No.	Property	FULC wall*	Normal brick wall
1	Thermal conduction coefficient, W/(m.K)	0.380	1.25
2	Specific heat, J/(kg.K)	0.85	0.92
3	Density, kg/m^3	716	2090
4	Convection coefficient, W/(m^2.K)	25	25

*FULC − foamed ultra-lightweight composite

Furthermore, the thermal conductivity of the FULC wall was compared with that of the normal brick wall under fire conditions to evaluate the thermal characteristics of FULC. It is noted that normal brick is one of the most popular and widely used construction materials in Vietnam. Therefore, it is chosen for the comparison with the FULC in order to demonstrate the advantages of using FULC instead of normal brick in terms of thermal behavior.

3. Results and Discussion

3.1. Compressive strength

Compressive strength development of the FULC specimens with various FA/GGBFS ratios is shown in Fig. 6. It can be seen that the FA/GGBFS ratio affected the compressive strength of FULC. The higher the FA/GGBFS ratio, the lower the compressive strength, regardless of age curing. There was an increase in the compressive strength of FULC when using the smaller amount of FA and higher amount of GGBFS (i.e., the higher FA/GGBFS ratio). The increase in compressive strength was due to the existence of FA and GGBFS, which filled the voids between grains and contributed to the better size distribution of the matrix, resulting in a reduction of porosity (as can be observed in Fig. 8) and thereby, improving compressive strength [24, 25]. In addition, Wang et al. [24] and Tangpagasit et al. [26] previously reported that the reactions between reactive SiO_2 and Al_2O_3 available in source materials and $Ca(OH)_2$ formed from cement hydration created secondary hydration products such as C–S–H and C–A–S–H. The amount of these products increased over time, and they filled voids inside FULC, resulting in the denser structure. This may be a possible explanation for the strength results obtained in the present study.

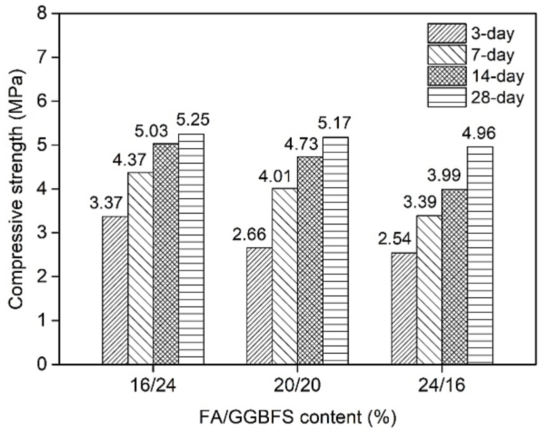

Figure 6. Compressive strength development of the FULC specimens with various FA/GGBFS ratios.

In general, the use of a higher amount of foam negatively affects the compressive strength of the FULC specimens, especially at the early ages [27]. The effect of F/W ratios on the compressive strength of FULC specimens is shown in Fig. 7. The high amount of foam (i.e., the low F/W) decreased the compressive strength of FULC. This behavior was due to an increase of void volume and the negative influence of foam on the pore size distribution and the quality of binding skeleton, resulting in a decrease in the final strength of the porous matrix [28, 29].

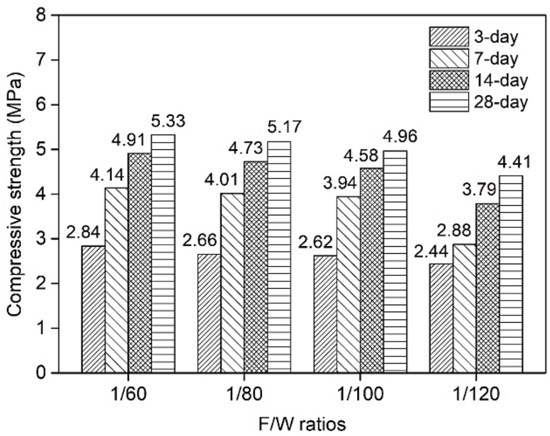

Figure 7. Compressive strength development of the FULC specimens with different F/W ratios.

3.2. Microstructure

The microstructure of FULC samples was shown in Fig. 8 by using a scanning electron microscopy technique (SEM). As seen in Fig. 8(a), M1 remained the unreacted GGBFS particles with angular shapes that formed the non-homogeneity structure inside the FULC specimen. The appearance of GGBFS and a suitable superplasticizer decreased air-void spaces and narrowed air-void size distributions [30]. Fig. 8(c) shows that the higher amount of unreacted FA particles. It indicates that FA played a role as an inert component, instead of pozzolanic material. The filler role of FA resulted in a more uniform distribution of pores and prevented from merging and overlapping of pores at higher foam content [31].

In addition, the air-void spaces were formed when adding the high amount of foam to FULC specimens, as shown in Fig. 8(b), (d), (e), and (f). The expansion of internal pores volume gradually exposed as seen in Fig. 8(d), (b), (e), and (f) with the use of F/W at the levels of 1/60, 1/80, 1/100, and 1/120, respectively. Thus, the inclusion of foam restructured and changed characteristics through the formation of bubbles inside the FULC specimen. It leads to increase porosity and thus minimize TC property of the FULC. The previous research proved that the properties of foam concrete have no relation with air-void shape because of the approximately same shape of all air voids and independence of foam volume [31]. Cebeci [32] also proved that the large voids do not change the characteristics of the fine pore structure of hardened cement paste. Moreover, it is found that the amount of foaming agent used affected not only the physical properties but also the production cost of the FULC.

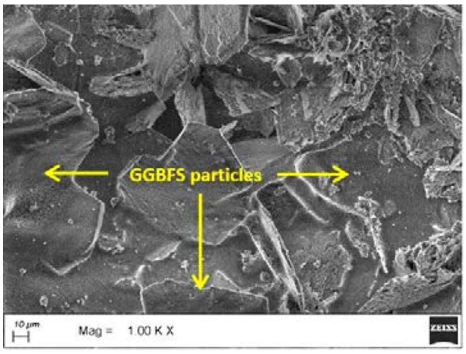

(a) M1

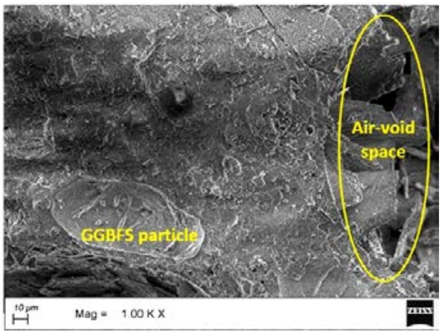

(b) M2

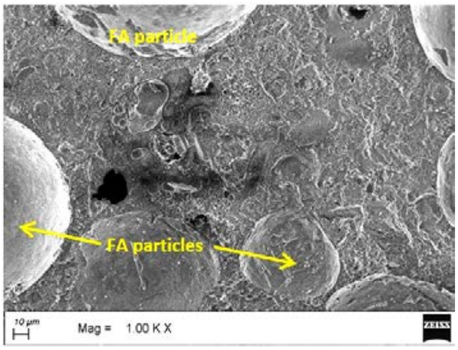

(c) M3

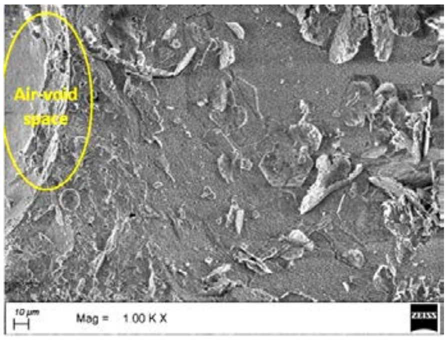

(d) M4

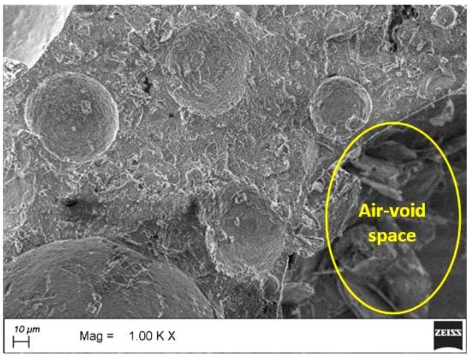

(e) M5

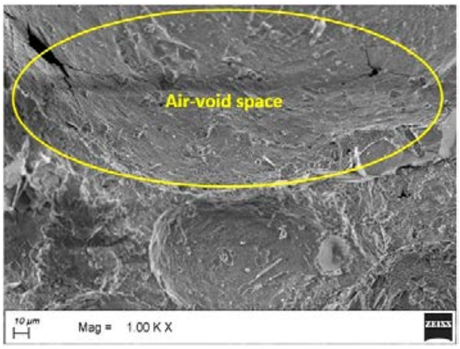

(f) M6

Figure 8. SEM images of the FULC specimens at 28 days.

3.3. Dry density and water absorption

Table 4 lists the engineering properties of FULC mixtures. The density of all of the FULC specimens was in the range of 716–728 kg/m³. The higher the foam amount, the lower the density of FULC. The inclusion of foam released air-entrapped parts leaving the void spaces and increased the porosity inside the FULC structure. As a result, the density of FULC specimens reduced, and their water absorption increased. Moreover, the introduction of foam leads to the reduction of FULC production cost significantly from 20.9 USD/m³ for FULC with F/W = 1/60 to 15.3 USD/m³ for FULC with F/W = 1/120 (Table 4).

Table 4. Engineering properties of the FULC specimens.

Mixtures	Dry density (kg/m³)	Thermal conductivity (W/mK)		Water absorption (%)	Cost (USD/m³)
		SSD*	OD**		
M1	726	0.454	0.178	44.4	18.6
M2	721	0.445	0.175	45.7	18.0
M3	717	0.438	0.168	46.9	17.5
M4	728	0.495	0.182	41.5	20.9
M5	719	0.441	0.171	46.7	15.6
M6	716	0.380	0.163	48.5	15.3

*SSD – saturated surface dry condition; **OD – oven dry condition

Although it can be seen the relationship between the dry density of the FULC and its compressive strength and water absorption rate through the data provided in Table 4 and Fig. 6 and 7, these relationships are clearly displayed in Fig. 9 and 10.

Fig. 9 shows the relationship between dry density and compressive strength. It can be expressed by equation (3) with R^2 = 0.93:

$$y = 1248.4 - 232.6x + 25.3x^2. \quad (3)$$

It is reasonable that the higher dry density of the FULC was proportional to its higher compressive strength value. As aforementioned, the lower the amount of foam in the FULC mixtures, the lower the porosity of the FULC samples. Thus, the denser structure of the FULC samples resulted in the higher dry density, which consequently leads to the higher compressive strength of the FULC samples, as can be seen in Fig. 9.

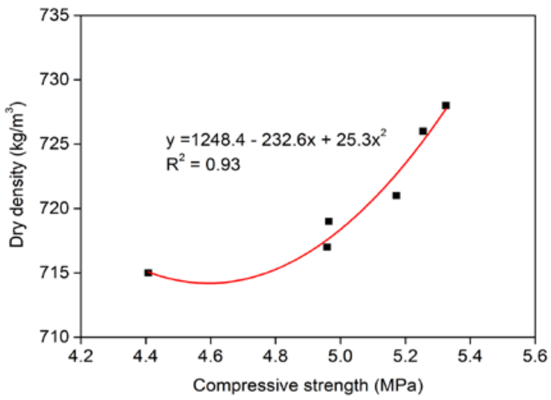

Figure 9. The relationship between dry density and compressive strength of the FULC specimens at 28 days.

Moreover, Fig. 10 shows the relationship between dry density and water absorption. There was an adverse relationship between dry density and water absorption, as shown in a representative equation (4) with R^2 = 0.91:

$$y = 523.2 + 10.9x - 0.14x^2. \quad (4)$$

The negative correlation is due to the characteristics of FA, whose crystal contained a considerable amount of quartz phase. Hence, the involvement of FA in the chemical reaction of the system is limited and thus releasing the gaps inside the FULC structure. The excessive addition of foaming agent commonly created air-voids and thereby, resulting in the low density and the low compressive strength [31]. Furthermore, the air-void parameters, including volume, size, and spacing, influenced strength and density [31]. It was also found that the air-void size distribution is one of the essential micro-properties affecting the strength of foam concrete [33].

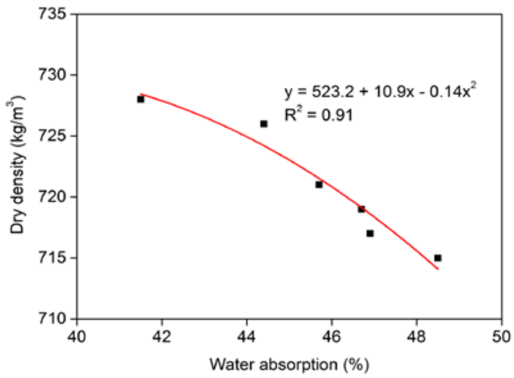

Figure 10. The relationship between dry density and water absorption of the FULC specimens at 28 days.

3.4. Thermal conductivity

The 28-day TC values recorded for the FULC specimens at both saturated-surface-dry (SSD) and oven-dry (OD) conditions are given in Table 4.

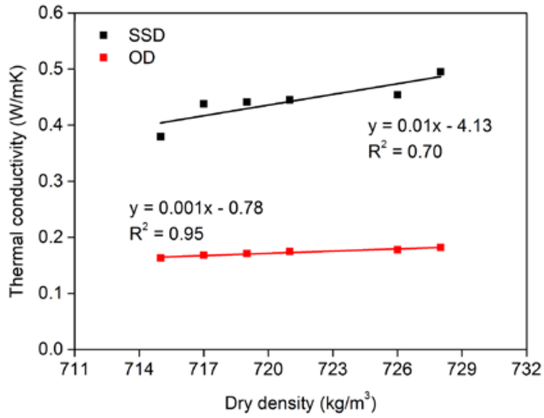

Figure 11. The relationship between dry density and thermal conductivity of the FULC specimens at 28 days.

As the results, the TC values were in the range of 0.380–0.495 W/(m.K) and 0.163–0.182 W/(m.K) for the FULC specimens in SSD and OD conditions, respectively. Thus, the SSD-TC of the FULC specimens was about 2.5 times higher than the OD-TC of the FULC specimens. This finding is supported by the previous results reported by Kim et al. [34] as the TC was proportional to the moisture of the specimens. The TC results from Table 4 also reveal that the effect of FA/GGBFS ratios on the TC of the FULC specimens was less significant than the impact of F/W ratios TC of the FULC specimens. Papa et al. [35] previously reported that higher void volume resulted in lower TC of the material. On the other hand, Fig. 11 shows the linear correlation between TC and the dry density of FULC specimens at the age of 28 days as higher dry density was associated with higher TC values.

3.5. The behavior of FULC under fire condition

To create the finite element models in ANSYS APDL software, multiple tasks have to be completed for the model to run correctly. In this thermal model plane, 55 was used for the wall. This element is available in the elements library of ANSYS APDL, as shown in Fig. 12.

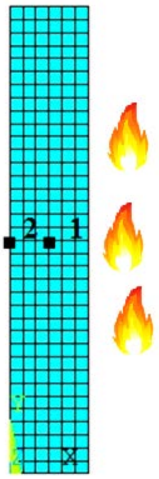

Figure 12. Finite element model.

Temperature distribution in the wall exposed to fire depended on space and time. The temperature of the points (Node 1 – the center of the wall and Node 2 – the inside surface of the wall) for the two types of walls, including the FULC wall and normal brick wall, was analyzed as shown in Fig. 13.

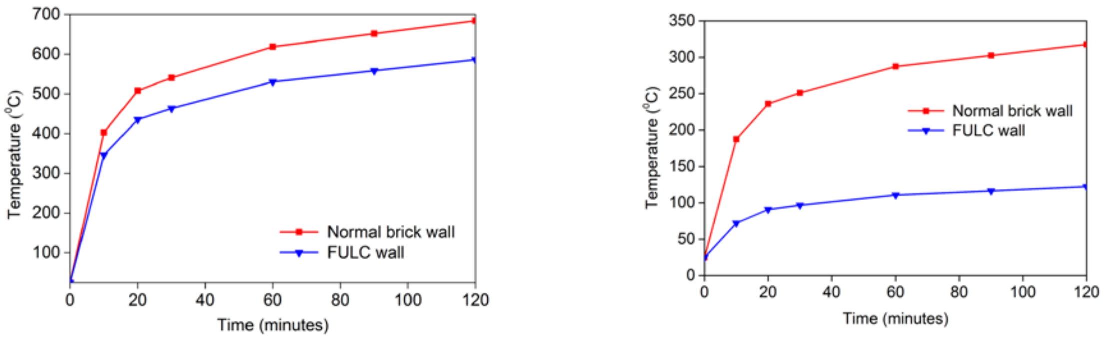

a. Node 1 **b. Node 2**

Figure 13. The temperature at Node 1 (a) and Node 2 (b) in the FULC wall and normal brick wall.

It is easy to observe the difference of temperature distribution between the center (Node 1) and outer points (Node 2) of the FULC wall and the normal brick wall. After 120 minutes of fire, the variation of maximum temperature at the center and surface of the normal wall brick and the FULC wall was 14.30 % and 61.49 %, respectively. As expected, the FULC wall had better insulation performance than the normal wall brick. This behavior is in good agreement with the result of the TC test.

4. Conclusions

The feasibility of the use of a ternary mixture of cement, GGBFS, and FA for producing FULC was investigated in this study. The mechanical and thermal properties of FULC were further evaluated. The following conclusions can be made based on the experimental outcomes:

1. 28-day compressive strength of the FULC ranged from 4.41 to 5.33 MPa, which can be classified as Grade 5.0 of foamed lightweight concrete as stipulated by TCVN 9029–2017 Vietnamese standard. There was an increase in the compressive strength of the FULC (from 4.96 MPa to 5.25 MPa) when using the lower amount of FA and a higher amount of GGBFS. Moreover, the inclusion of a higher amount of foam negatively affected the compressive strength of the FULC specimens as the reduced strength from 5.33 MPa to 4.41 MPa was observed.

2. Dry density and water absorption of the FULC at 28 days were in the ranges of 716–729 kg/m3 and 41.5–48.5 %, respectively. The higher the foaming agent amount, the lower the density, and the higher the water absorption rate of the FULC.

3. After 28 days, the thermal conductivity of the FULC in SSD and OD conditions were in the ranges of 0.380–0.495 and 0.163–0.182 W/mK, respectively. The inclusion of more foam resulted in more void volume and thus lower TC value. Foam contributed to the comfort of the building by lowering thermal

transfer. Furthermore, it is interesting to find that the effect of FA/GGBFS ratios on the TC of the FULC specimens was less significant than the effect of F/W ratios TC of the FULC specimens.

4. After 120 minutes under fire, the maximum temperature at the center of the FULC wall and the normal brick wall was 317.7 and 122.30 °C, respectively. Whereas, the maximum temperature at the outer surface of the FULC wall and the normal brick wall was 684.0 and 586.20 C, respectively. Thus, The FULC exhibited better performance under fire conditions in comparison with the normal brick.

5. It could be observed from the SEM images of the FULC specimens that the air-void spaces were formed when adding a high amount of foam to FULC specimens. On the other hand, the foam not only affected the physical properties of FULC but also lowered the cost for the production of FULC when taking into account the effectiveness of optimization of the content of the use of a foaming agent. The material cost of the FULC mixtures ranged from 15.3−20.9 USD/m3.

6. Consequently, industrial waste products such as GGBFS and FA can be potentially used for the production of FULC. In future work, the characteristic of FULC incorporating various types of waste materials should be investigated to enhance the background of the present study.

5. Acknowledgment

The authors would like to express the sincere thanks to Huynh's research group at Can Tho University, Vietnam, for their kind assistance provided during the experimental works.

References

1. Othuman, M.A., Wang, Y.C. Elevated-temperature thermal properties of lightweight foamed concrete. Construction and Building Materials. 2011. 25(2). Pp. 705–716.
2. Kerali, A.G. Durability of compressed and cement-stabilised building blocks. [Online]. System requirements: AdobeAcrobatReader. URL: https://pdfs.semanticscholar.org/0796/d37441d7120d683f0388c40c4e557ef248ad.pdf (date of applica-tion: 13.08.2019).
3. Kumar, N.V., Arunkumar, C., Senthil, S.S. Experimental study on mechanical and thermal behavior of foamed concrete. Materials Today: Proceedings. 2018. 5(2). Pp. 8753–8760.
4. Mydin, M.A.O., Wang, Y.C. Mechanical properties of foamed concrete exposed to high temperatures. Construction and Building Materials. 2012. 26(1). Pp. 638–654.
5. Lim, S.K., Tan, C.S., Lim, O.Y., Lee, Y.L. Fresh and hardened properties of lightweight foamed concrete with palm oil fuel ash as filler. Construction and Building Materials. 2013. 46. Pp. 39–47.
6. Pacheco-Torgal, F. Eco-efficient construction and building materials research under the EU Framework Programme Horizon 2020. Construction and Building Materials. 2014. 51. Pp. 151–162.
7. Zhang, Z., Provis, J.L., Reid, A., Wang, H. Geopolymer foam concrete: An emerging material for sustainable construction. Construction and Building Materials. 2014. 56. Pp. 113–127.
8. Jones, M.R., McCarthy, A. Preliminary views on the potential of foamed concrete as a structural material. Magazine of Concrete Research. 2005. 57(1). Pp. 21–31.
9. Korniyenko, S.V., Vatin, N.I., Gorshkov, A.S. Thermophysical field testing of residential buildings made of autoclaved aerated concrete blocks. Magazine of Civil Engineering. 2016. 4. Pp. 10–25.
10. Korniyenko, S.V. Advanced hygrothermal performance of building component at reconstruction of S. Radonezhskiy temple in Volgograd, MATEC Web of Conferences. 2016. 53.
11. Olivier, J.G., Maenhout, G.J., Muntean, M., Peters, J.A.H.W. Trends in global CO_2 emissions: 2016 report. [Online]. System requirements: Adobe Acrobat Reader. URL: https://www.pbl.nl/sites/default/files/cms/publicaties/pbl-2016-trends-in-global-co2-emisions-2016-report-2315.pdf (date of application: 13.08.2019).
12. Mikulčić, H., Klemeš, J.J., Vujanović, M., Urbaniec, K., Duić, N. Reducing greenhouse gasses emissions by fostering the deployment of alternative raw materials and energy sources in the cleaner cement manufacturing process. Journal of Cleaner Production. 2016, 136. Pp. 119–132.
13. Gowri, R., Anand, K.B. Utilization of fly ash and ultrafine GGBS for higher strength foam concrete. IOP Conference Series: Materials Science and Engineering. 2018. 310.
14. Nambiar, E.K.K., Ramamurthy, K. Influence of filler type on the properties of foam concrete. Cement and Concrete Composites. 2006. 28(5). Pp. 475–480.
15. Hwang, C.L., Huynh, T.P. Effect of alkali-activator and rice husk ash content on strength development of fly ash and residual rice husk ash-based geopolymers. Construction and Building Materials. 2015. 101. Pp. 145–155.
16. Hwang, C.L., Tran, V.A. Engineering and durability properties of self-consolidating concrete incorporating foamed lightweight aggregate. Journal of Materials in Civil Engineering. 2016. 28(9).
17. Oluwole, O., Joshua, J., Nwagwo, H. Finite element modeling of low heat conducting building bricks. Journal of Minerals and Materials Characterization and Engineering. 2012. 11. Pp. 800–806.
18. Nguyen, T.C., Luu, X.B. Reducing temperature difference in mass concrete by surface insulation. Magazine of Civil Engineering. 2019. 88(4). Pp. 70–79.

19. Lam, T.V., Nguyen, T.C., Bulgakov, B.I., Anh, P.N. Composition calculation and cracking estimation of concrete at early ages. Magazine of Civil Engineering. 2018. 82(6). Pp. 136–148.
20. Chuc, N.T., Lam, T.V., Bulgakov, B.I. Designing the composition of concrete with mineral additives and assessment of the possibility of cracking in cement-concrete pavement. Materials Science Forum. 2018. 931. Pp. 667–673.
21. Fakury, R.H., Casas, E.B.L., Júnior, F.P.F., Abreu, L.M.P. Numerical analysis of the Eurocode assumptions for temperature distribution in composite steel and concrete beams. Mecánica Computacional. 2002. XXI. Pp.1998–2008.
22. Jacob, B., Balaji, A., John. E. Behaviour of concrete structures under fire - a comparative study between IS 456: 2000 and finite element software ANSYS. American Journal of Engineering Research. 2013. 3. Pp. 62–66.
23. Casano, G., Piva, S. Transient heat conduction in a wall exposed to a fire: an analytic approach. Journal of Physics: Conference Series. 2017. 796(1). 11 p.
24. Wang, A., Zhang, C., Sun, W. Fly ash effects: III. The micro aggregate effect of fly ash. Cement and Concrete Research. 2004. 34(11). Pp. 2061–2066.
25. Aghaeipour, A., Madhkhan, M. Effect of ground granulated blast furnace slag (GGBFS) on RCCP durability. Construction and Building Materials. 2017. 141. Pp. 533–541.
26. Tangpagasit, J., Cheerarot, R., Jaturapitakkul, C., Kiattikomol, K. Packing effect and pozzolanic reaction of fly ash in mortar. Cement and Concrete Research. 2005. 35(6). Pp. 1145–1151.
27. Kearsley, E.P., Wainwright, P.J. The effect of high fly ash content on the compressive strength of foamed concrete. Cement and Concrete Research. 2001. 31(1). Pp. 105–112.
28. Kearsley, E.P., Wainwright, P.J. The effect of porosity on the strength of foamed concrete. Cement and Concrete Research. 2002. 32(2). Pp. 233–239.
29. Hajimohammadi, A., Ngo, T., Mendis, P., Kashani, A., van Deventer, J.S.J. Alkali activated slag foams: The effect of the alkali reaction on foam characteristics. Journal of cleaner production. 2017. 147. Pp. 330–339.
30. Jiang, J., Lu, Z., Niu, Y., Li, J., Zhang, Y. Study on the preparation and properties of high-porosity foamed concretes based on ordinary Portland cement. Materials & Design. 2016. 92. Pp. 949–959.
31. Nambiar, E.K.K., Ramamurthy, K. Air-void characterisation of foam concrete. Cement and Concrete Research. 2007. 37(2). Pp. 221–230.
32. Cebeci, O.Z. Pore structure of air-entrained hardened cement paste. Cement and Concrete Research. 1981. 11(2). Pp. 257–265.
33. Kearsely, E.P., Visagie, M. Specialist techniques and materials for construction. 1999. 11 p.
34. Kim, K.H., Jeon, S.E., Kim, J.K., Yang, S. An experimental study on thermal conductivity of concrete. Cement and Concrete Research. 2003. 33(3). Pp. 363–371.
35. Papa, E., Medri, V., Kpogbemabou, D., Morinière, V., Laumonier, J., Vaccari, A., Rossignol, S. Porosity and insulating properties of silica-fume based foams. Energy and Buildings. 2016. 131. Pp. 223–232.

Contacts:

Trong-Phuoc Huynh, htphuoc@ctu.edu.vn
Nguyen-Trong Ho, ntrong.ho@gmail.com
Phuong-Trinh Bui, buiphuongtrinh@hcmut.edu.vn
Ngoc-Duy Do, dongocduy29@gmail.com
Trong-Chuc Nguyen, ntchuc.mta198@gmail.com